

Neuronal Adaptation to a Constant Stimulus  
in the Hodgkin-Huxley Model

Austin Che  
Maya Barley

December 7

### Abstract

When stimulated continuously by a holding current, a neuron shows *adaptation*: it becomes increasingly difficult to produce an action potential. This phenomenon is exhibited in the giant squid axon. Using the Hodgkin-Huxley space-clamped simulation software, we varied the holding current and determined the minimum amplitude of a pulse needed for the membrane potential to reach the sodium Nernst potential. The results showed three distinct regions of behavior. For negative holding currents, there was a linear inverse relationship between the stimulus amplitude and the holding current. For positive holding currents less than  $1164\mu\text{A}/\text{cm}^2$ , the required stimulus amplitude increased. For larger values of holding current, the stimulus required began to decrease. This complex behavior was explained using the Hodgkin-Huxley model. A continuously applied holding current changes the resting membrane potential, shifting the equilibrium points corresponding to the resting potential, threshold, and the peak of an action potential.

# Contents

<b>1</b>	<b>Introduction</b>	<b>3</b>
1.1	The Hodgkin-Huxley Model . . . . .	3
1.2	Equilibrium Points . . . . .	3
1.3	Hypothesis . . . . .	5
<b>2</b>	<b>Methods</b>	<b>5</b>
2.1	Simulation Setup . . . . .	5
2.2	Measuring Neuronal Adaptation . . . . .	6
2.3	Manipulating the HH Software . . . . .	7
2.4	Understanding the Hodgkin-Huxley Mechanism . . . . .	7
<b>3</b>	<b>Results</b>	<b>7</b>
3.1	Resting Membrane Potential v. Holding Current . . . . .	7
3.2	The $J_p$ v. $J_h$ Relationship . . . . .	8
3.3	Hodgkin-Huxley Parameters . . . . .	9
3.3.1	Region A . . . . .	10
3.3.2	Region B . . . . .	11
3.3.3	Region C . . . . .	12
<b>4</b>	<b>Discussion</b>	<b>12</b>
4.1	Explaining Adaptation . . . . .	12
4.1.1	Inadequacies of the Equilibrium Points Model . . . . .	12
4.1.2	Region A . . . . .	13
4.1.3	Region B . . . . .	14
4.1.4	Region C . . . . .	14
4.2	Verifying Results with PAP Software . . . . .	15
4.3	Controls . . . . .	15
4.4	Future Work . . . . .	16
4.4.1	Software . . . . .	16
4.4.2	Action Potential Definitions . . . . .	17
4.5	Conclusion . . . . .	17
<b>Appendix A: Software Script</b>		
<b>Appendix B: Sample Waveforms</b>		
<b>Appendix C: Project Proposal</b>		

# 1 Introduction

## 1.1 The Hodgkin-Huxley Model

The Hodgkin-Huxley (HH) model describes the neuronal membrane in terms of ionic conductances, Nernst potentials, and a capacitive component. The sodium conductance depends on the values of  $m$  and  $h$ , the activation and inactivation factors, that in turn depend on the membrane potential:

$$G_{Na}(V_m, t) = \overline{G_{Na}} m^3(V_m, t) h(V_m, t). \quad (1)$$

Likewise, the potassium conductance is related to the value of  $n$ , the voltage-dependent potassium activation factor:

$$G_K(V_m, t) = \overline{G_K} n^4(V_m, t). \quad (2)$$

The factors  $m$ ,  $n$ , and  $h$  are all exponentials, with asymptotic values and time constants satisfying the following equation:

$$x(t) = x_\infty(V_m) - (x_\infty(V_m) - x_0) e^{-t/\tau_x(V_m)}. \quad (3)$$

The  $x_\infty$  and  $\tau_x$  dependence on the membrane resting potential is given in Weiss [1].

## 1.2 Equilibrium Points

A plot of the capacitance current  $J_C$  versus the membrane potential gives insight into the mechanism generating action potentials. Because

$$J_C = C_m \frac{dV_m}{dt}. \quad (4)$$

the membrane potential can be at equilibrium, i.e. not changing, when  $J_C = 0$ . We can plot  $J_C$  by plotting  $J_{ion}$ , because  $J_C = -J_{ion}$ . In addition,  $m$  is assumed to be very fast so that  $m$  is always equal to  $m_\infty(V_m)$ . We also assume that  $n$  and  $h$  are so slow that their values are fixed at  $n_\infty(V_m^o)$  and  $h_\infty(V_m^o)$  respectively. A typical plot is shown in Figure 1. The top plot shows the general shape of the curve and the bottom plot magnifies the region near  $J_{ion} = 0$ .

Three equilibrium points exist, corresponding to  $J_{ion} = -J_C = 0$ . The first equilibrium point occurs at the resting membrane potential  $V_m^o$ , the second

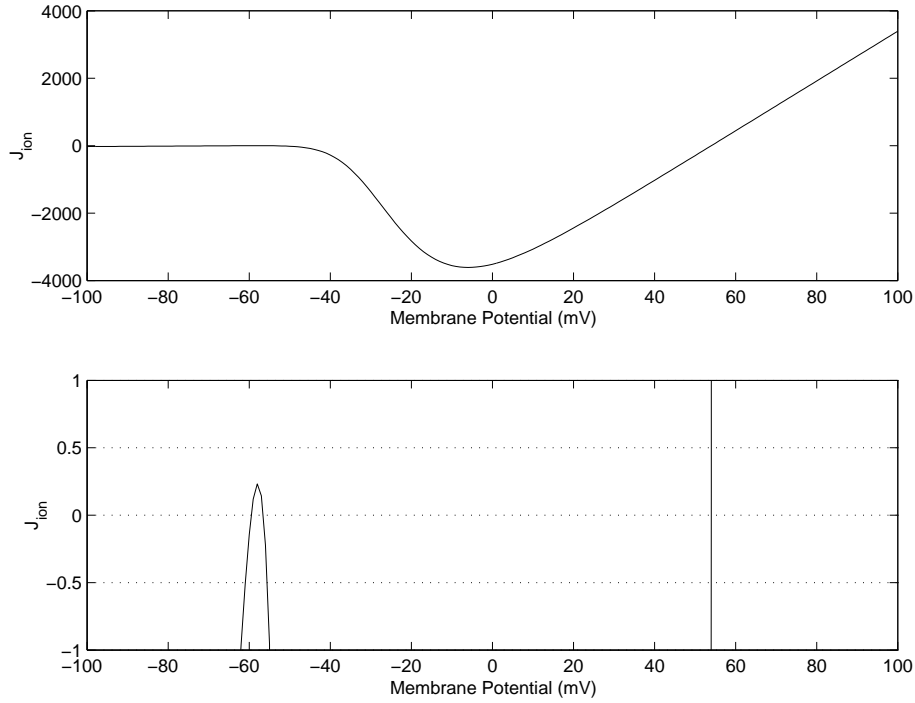


**Figure 1:** A plot of  $J_{ion}$  versus membrane potential assuming  $m$  is very fast and changes instantly, and  $n$  and  $h$  are very slow and stay at their original values. Plotting  $J_{ion}$  on a magnified scale (bottom plot) shows that  $J_{ion}$  is zero for 3 values of  $V_m$ : two near  $V_m = -60\text{mV}$  and one near  $V_m = +55\text{mV}$ .

at the threshold (slightly higher than rest), and the third near the sodium Nernst potential. The first and third equilibrium points are stable, in that the membrane potential will move back to these points after being perturbed slightly. On the other hand, the threshold equilibrium point is unstable. A small voltage deviation will create a regenerative effect, pushing the potential in the direction of the original deviation.

As a result of this behavior, to transition between the first and third equilibrium points (i.e. to generate an action potential), the membrane voltage need only be perturbed just beyond the threshold voltage.

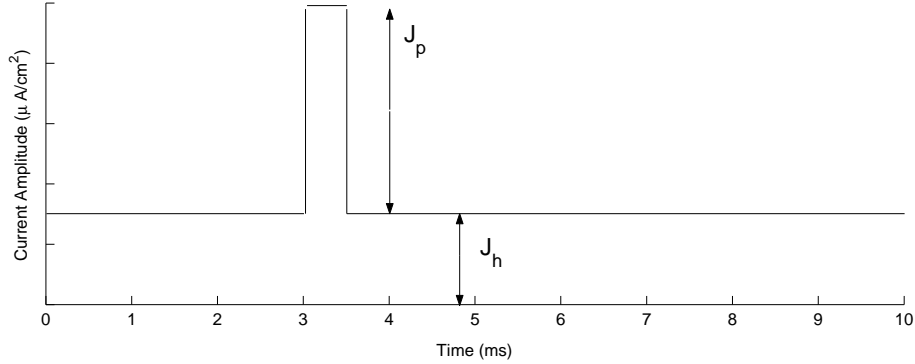


**Figure 2:** The stimulating current consisted of a holding current ( $J_h$ ) and a short current pulse ( $J_p$ ).

### 1.3 Hypothesis

When a neuron is stimulated continuously by a current of constant intensity (a holding current), it becomes harder to generate an action potential with a pulse. This property is called *adaptation*. Higher holding currents depolarize the membrane to greater degrees, causing the resting potential,  $V_m^o$ , to increase.

In the Hodgkin-Huxley model, based on the shape of the sigmoidal  $m_\infty$  curve and the  $\tau_m$  curve, at higher values of  $V_m^o$ , the initial value of  $dm/dt$  would be smaller, and so it would be harder to generate an action potential.

Consequently, we hypothesized that the larger the holding current, the larger the current pulse amplitude required to elicit an action potential in the Hodgkin-Huxley model.

## 2 Methods

### 2.1 Simulation Setup

We performed simulations using the HH space-clamped model with a stimulus comprised of a holding current with amplitude  $J_h$  followed by a short rectangular current pulse with fixed duration 0.5ms and amplitude  $J_p$  (see Figure 2).

The space-clamped software was used instead of the propagating action potential model, because the space-clamped software begins the simulation with all variables already in the steady-state, under the assumption that the holding

current has been applied since  $t = -\infty$ . It was desirable for all variables to be in steady-state at the instant before the stimulating pulse, because we did not wish to consider the transient effects of applying the holding current. Furthermore, in the propagated action potential software, the holding current is only applied at one point on the axon. The purpose of this experiment was to look at the effects when a holding current is applied along the *entire* axonal length (a current clamp).

## 2.2 Measuring Neuronal Adaptation

We measured the smallest amplitude of the pulse needed to generate an action potential. The occurrence of an action potential was defined as when  $V_m$  reached a maximum value,  $V_{max}$ , equal to the sodium Nernst potential, or about 55 mV. This definition was chosen because the peak of an action potential will approach this value. The space-clamp method eliminates propagation, and therefore we could not use decrement-free propagation as a measure of the occurrence of an action potential. To check our results were not dependent upon this definition, we also ran simulations using the following definitions to see if they produced dramatically different outcomes:

- $V_{max} - V_m^o > 50\text{mV}$ . An action potential has a characteristically large voltage range. If the maximum of the potential reached at least 50mV above the resting potential, we took it as a positive sign of the occurrence of an action potential.
- $V_{max} > V_{Na} - 20\text{mV}$ . The peak of an action potential is determined by a weighted sum of the sodium and potassium Nernst potentials. Therefore, the peak produced by a threshold stimulus is unlikely to reach  $V_{Na}$ ; using  $V_{Na} - 20\text{mV}$  may be more accurate.
- $V_{min} < V_m^o$ . An action potential has a characteristic hyperpolarization before returning to rest. We therefore would expect an action potential waveform to have a minimum value less than the resting potential.

After running simulations using each definition in turn, we defined an action potential as one that satisfied all three criteria.

Measurements were made for holding currents from  $-100\mu\text{A}/\text{cm}^2$  to  $4000\mu\text{A}/\text{cm}^2$  in increments of  $50\mu\text{A}/\text{cm}^2$ . This range was chosen because for holding currents

more negative than -100, the membrane potential becomes more negative than  $V_K$ , which is physiologically unrealistic. For holding currents larger than 4000, the membrane potential is greater than  $V_{Na}$ .

### 2.3 Manipulating the HH Software

Instead of manually collecting data, a collection of scripts (see Appendix A) was written to run the software. This was done for the following reasons:

- *Speed of data collection.* We needed to find the minimum amplitude of  $J_p$  required to generate a  $V_{max}$  greater than the sodium Nernst potential. Because this would have involved running many simulations for each holding current, we automated the process.
- *Calculating undisplayed parameters.* Potentially important values such as  $dm/dt$ ,  $dh/dt$ , and  $dn/dt$  are not accessible using the graphical interface. Using the script, all possible parameters can be calculated.
- *For data manipulation.* We wished to graph  $J_p$  and other parameters versus  $J_h$ . The software can only generate time-dependent graphs for a specific holding current.

### 2.4 Understanding the Hodgkin-Huxley Mechanism

After observing the relationship between  $J_p$  and  $J_h$ , we determined the Hodgkin-Huxley mechanism responsible for this behavior by plotting the following parameters versus the holding current: activation and inactivation factors, ionic conductances and currents, membrane potentials, and finally, ratios and differences among these variables. Also, for a range of holding currents, plots of  $J_C$  v. membrane potential were generated to determine the equilibrium points.

## 3 Results

### 3.1 Resting Membrane Potential v. Holding Current

As shown in Figure 3, the resting membrane potential,  $V_m^o$ , increases as the holding current increases. For negative holding currents, the membrane potential drops precipitously. This graph justifies the range of holding currents we used,

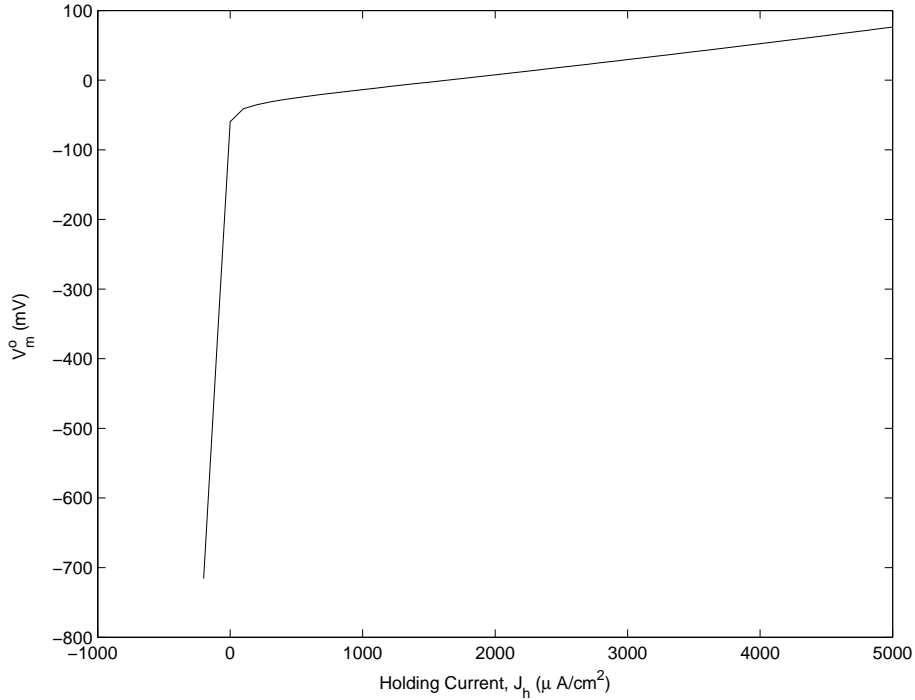


**Figure 3:** The resting membrane potential,  $V_m^o$ , is shown for different holding currents,  $J_h$ . As the holding current is increased, the resting membrane potential increases.

generating the range of resting membrane potentials approximately between the potassium and sodium Nernst potentials.

### 3.2 The $J_p$ v. $J_h$ Relationship

The minimum pulse amplitude  $J_p$  required to generate a  $V_{max}$  greater than the sodium Nernst potential is plotted for various values of the holding current  $J_h$  in Figure 4. The graph is clearly divided into three regions:  $J_h < 0$  (Region A),  $0 < J_h < 1164$  (Region B), and  $J_h > 1164$  (Region C).

- *Region A.*  $J_p$  decreases almost linearly with a steep slope as  $J_h$  increases. In Figure 4 the region around  $J_h = 0$  appears almost symmetrical, implying non-linear behavior. A plot of  $J_p$  v.  $J_h$  for the boundary between regions A and B is shown in Figure 5. This plot shows that the turnover

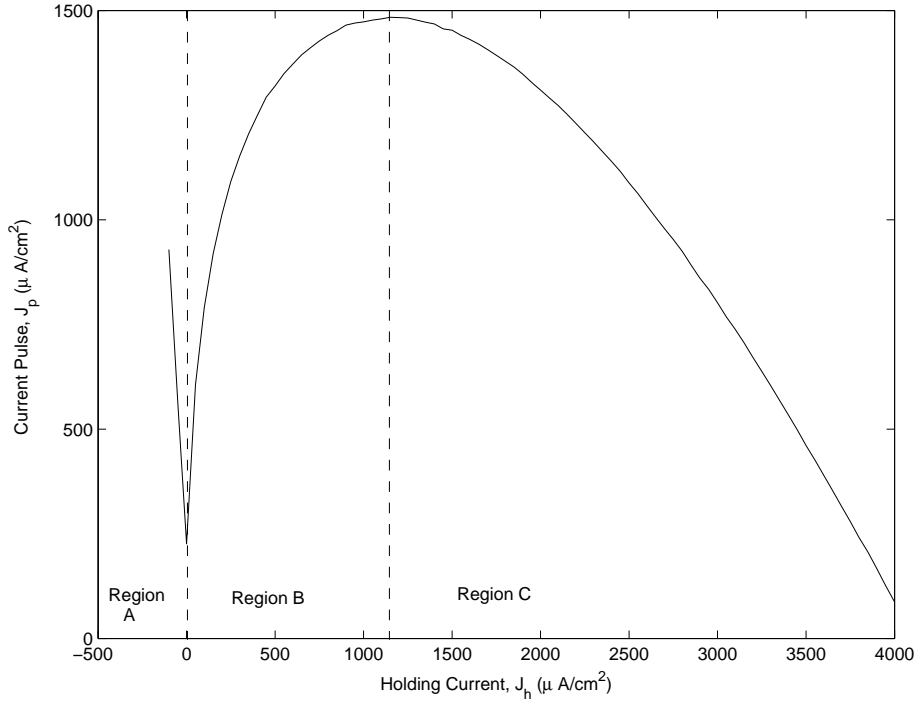


**Figure 4:** The pulse amplitude,  $J_p$ , needed to elicit an action potential is plotted for various holding currents,  $J_h$ . Distinctly different behaviors are seen in three regions, labelled A, B, and C.

point actually occurs at  $J_h < 0$  and is far smoother and more asymmetrical than Figure 4 suggests. A sample action potential waveform for  $J_h = -100 \mu\text{A}/\text{cm}^2$  is in Appendix B.

- *Region B.*  $J_p$  increases as  $J_h$  increases and the slope is decreasing, i.e.  $\frac{d^2 J_p}{dJ_h^2} < 0$ .
- *Region C.*  $J_p$  decreases as  $J_h$  increases and the slope is becoming more negative.

### 3.3 Hodgkin-Huxley Parameters

The Hodgkin-Huxley parameters for each region were analyzed separately due to the differing behaviors in regions A, B, and C. We used the method of analyzing equilibrium points by plotting  $J_C$  versus the membrane potential. Because

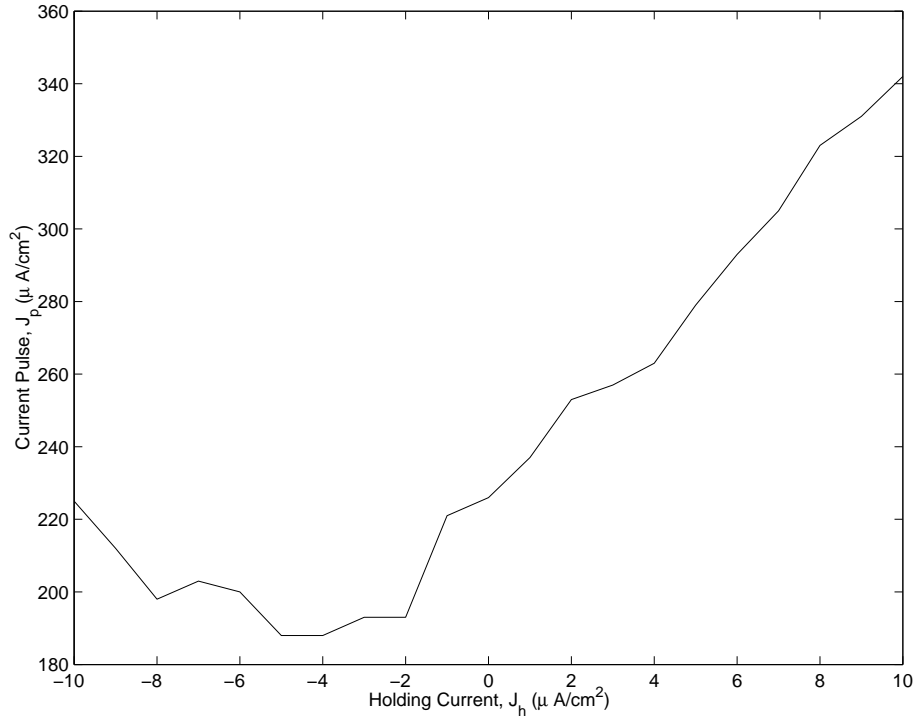


**Figure 5:** The pulse amplitude required to stimulate a nerve with a holding current near  $0\mu\text{A}/\text{cm}^2$ . The boundary between Region A and Region B is less distinct than in Figure 4.

$J_m = J_{ion} + J_C - J_h$ , and  $J_m = 0$  immediately after the pulse, we have that  $-J_C = J_{ion} - J_h$ . Thus, in the following graphs, we plot  $J_{ion} - J_h$  versus  $V_m$ .

### 3.3.1 Region A

To explain the behavior seen in Region A,  $J_{ion} - J_h$  values are plotted versus membrane potential in Figure 3.3.1 for several negative holding currents. The plot is zoomed in on the region around the origin. All the curves cross the horizontal zero axis at three points. The second and third crossings are essentially at the same membrane potential for all the curves. The only difference is in the location of the first equilibrium point, i.e. the resting membrane potential, which decreases approximately linearly as the holding current becomes more negative.

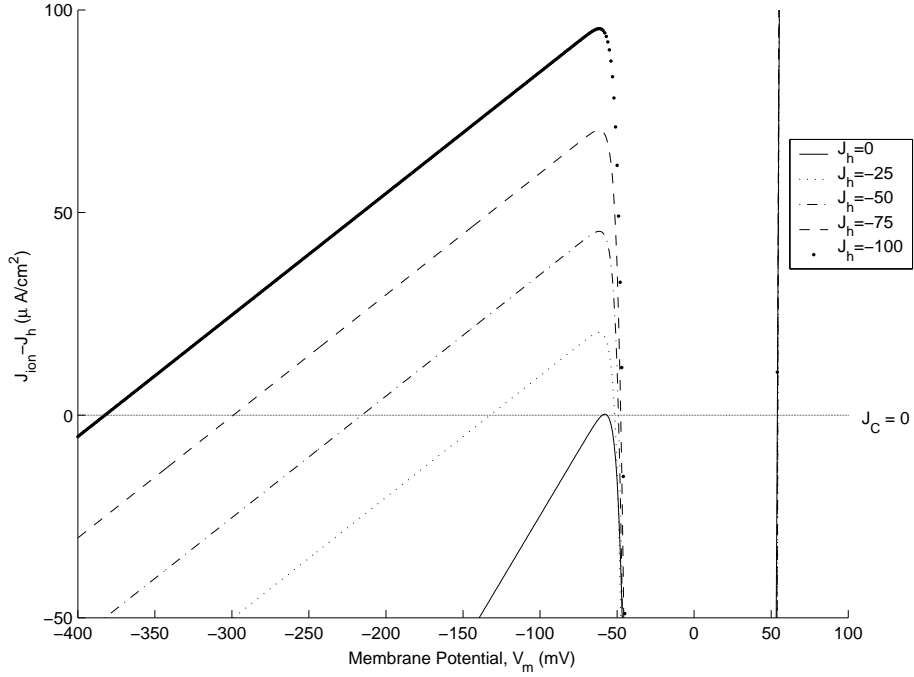


**Figure 6:** In Region A, the location of the first zero crossing becomes more negative as the holding current becomes more negative.

### 3.3.2 Region B

In Region B,  $0 < J_h < 1164$ , as the holding current is increased, a larger current pulse is needed to generate an action potential. Figure 7 shows the  $J_{ion} - J_h$  plot for holding currents in Region B. As the holding current increases, the sigmoidal shape of the curve becomes more linear.

In Figure 8, we magnify the region near zero to locate more precisely the equilibrium points for each of the curves. As  $J_h$  increases to about 250, the position of the third equilibrium point decreases. This third point roughly corresponds to  $V_{max}$  during an action potential. The second and third equilibrium points disappear when  $J_h$  increases beyond  $250 \mu A/cm^2$ . For even higher  $J_h$ , the curves become more linear and only the remaining equilibrium point corresponds to  $V_m^o$ .

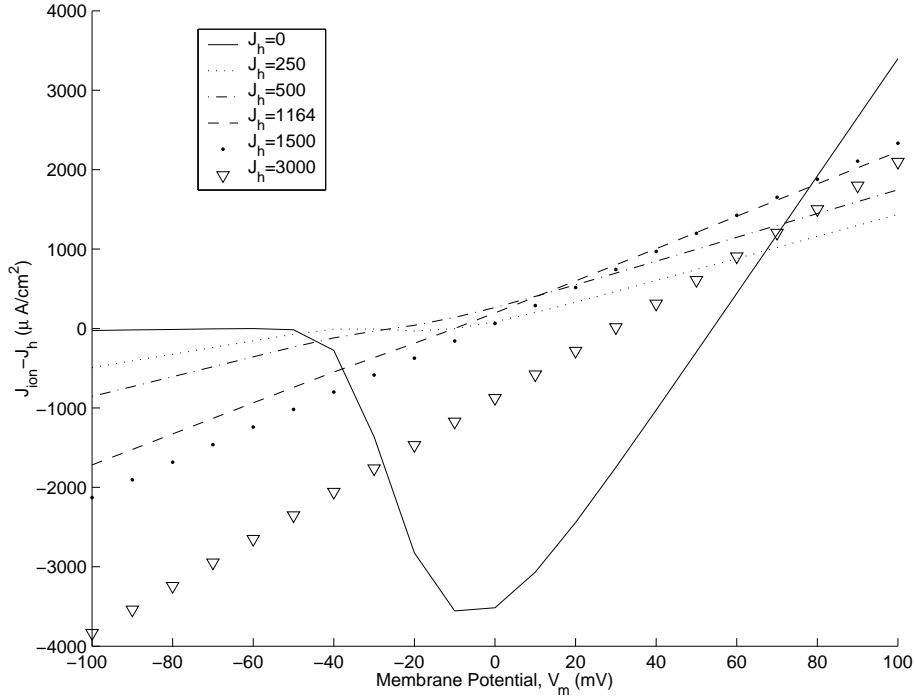


**Figure 7:** For positive holding currents, the shape of the  $J_{ion} - J_h$  curve becomes more linear as we increase the holding current.

### 3.3.3 Region C

Figures 7 and 8 also contain plots for holding currents in Region C. No obvious change occurs at the turnover point between Region B and Region C. A sample action potential waveform for  $J_h = 4000 \mu\text{A}/\text{cm}^2$  is in Appendix B.

## 4 Discussion

### 4.1 Explaining Adaptation

#### 4.1.1 Inadequacies of the Equilibrium Points Model

The model we used to plot  $J_C$  v.  $V_m$ , while valuable for analysis of the Hodgkin-Huxley mechanism, is only an approximation. If we took the model literally, it would be impossible to generate a voltage peak of greater than  $V_{Na}$ , because for any holding current, the third equilibrium point lies below  $V_{Na}$ . Nevertheless,

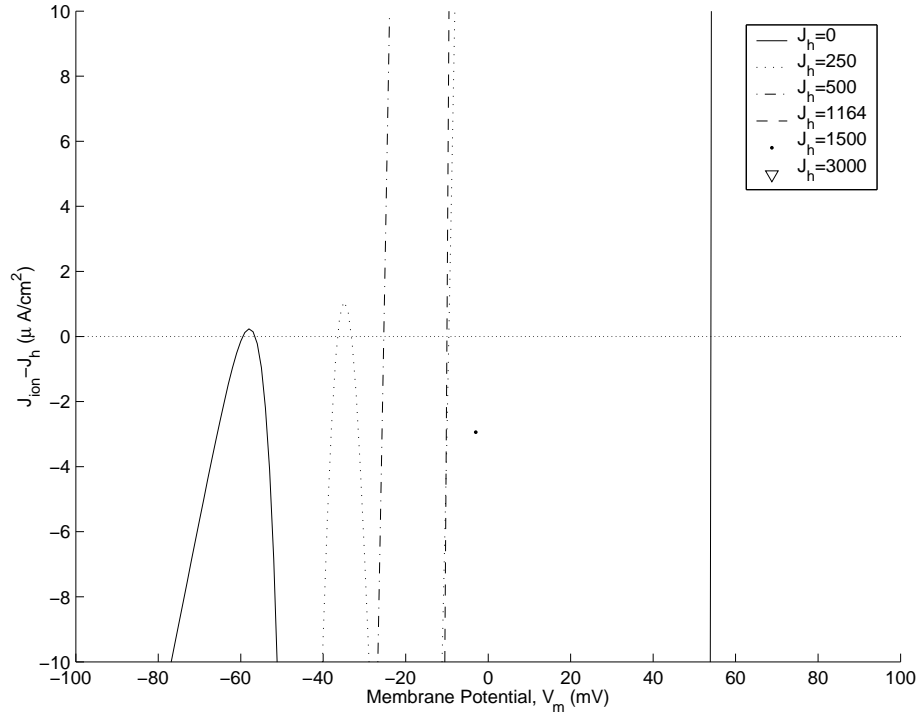


**Figure 8:** With increased  $J_h$ , all but one of the equilibrium points disappear.

the model gives us an idea about the underlying processes involved in the generation of action potentials in each region. Consequently, we will use it to explain our results, even though we should be wary of drawing too many conclusions from it.

#### 4.1.2 Region A

In Figure 3.3.1, as the holding current becomes more negative, the resting membrane potential decreases linearly, while the threshold point does not change significantly. Thus, a larger stimulus pulse is required to reach the threshold point and is in direct proportion to a more negative holding current. This linear relationship can explain the almost linear behavior seen in Figure 4 for Region A.

However, the action potential waveforms observed for negative values of  $J_h$  do not look like action potentials (see Appendix B). They have a much

slower repolarization, with a pronounced initial voltage spike, and they lack the characteristic post-action potential hyperpolarization. Therefore, our results for region A might be inaccurate in that we are *not* generating action potentials.

### 4.1.3 Region B

In Region B, as  $J_h$  increases slightly above 0, all three equilibrium points can still be seen in Figure 8. Although the first equilibrium point,  $V_m^o$ , increases, the last equilibrium point decreases. With  $V_{Na}$  being constant, the latter effect increases the membrane potential difference between  $V_{Na}$  and the maximum stable  $V_m$ . The greater the membrane potential is beyond this equilibrium point, the greater the  $J_{ion} - J_h$ . Because  $J_{ion} - J_h = -J_C = -C dV_m/dt$ , beyond the third equilibrium point,  $dV_m/dt$  is increasingly more negative. This makes it harder to reach  $V_{Na}$  as the membrane potential is drawn back towards the third equilibrium point.

For even larger values of  $J_h$ , the only stable equilibrium point exists at rest. The threshold equilibrium point disappears and there is no longer a metastable equilibrium voltage beyond which  $V_m$  experiences the positive feedback characteristic of the rising phase of an action potential. Therefore, according to this model, the stimulus, and *not* positive feedback, is the primary driving force on the membrane potential causing it to reach  $V_{Na}$ , and a larger stimulus will be required for  $V_{max}$  to reach  $V_{Na}$ . Even though this implies we are not generating an action potential, the model is only an approximation so threshold behavior might still exist. As shown in Appendix B, the waveforms produced in this region do have the appearance of an action potential.

### 4.1.4 Region C

The behavior in Region C is highly dependent on our definition of an action potential. Using our basic definition of  $V_{max} > V_{Na}$ , we observe the results shown in Figure 4. For  $J_h = 4000\mu\text{A}/\text{cm}^2$ ,  $V_m^o = 52.4\text{mV}$ , indicating an action potential voltage range of less than 3 mV (see Appendix B). Although the shape of the waveform is highly similar to an action potential, it is highly dubious that this waveform would be capable of decrement-free propagation. Therefore, we may not be generating an action potential.

On the other hand, using the combined definition of  $V_{max} - V_m^o > 50\text{mV}$ ,  $V_{max} > V_{Na}$ , and  $V_{min} < V_m^o$  we initially observe a slight downturn in  $J_p$  for

$J_h > 1164\mu\text{A}/\text{cm}^2$ . For  $J_h > 1800\mu\text{A}/\text{cm}^2$ ,  $J_p$  increases.

Our results for Region C depend on how the action potential is defined indicating that the results are probably *due* to this definition. As  $V_m^o$  increases towards  $V_{Na}$  in Region C, the stimulus needed for  $V_{max}$  to reach  $V_{Na}$  will become smaller. Thus, it could be due to our action potential definition that  $J_p$  decreases with increasing  $J_h$  in Region C, and not because of a Hodgkin-Huxley mechanism. As we are unsure of which action potential definition is more accurate, and we feel that all our definitions are reasonable, we are unable to describe the absolute behavior in Region C.

## 4.2 Verifying Results with PAP Software

To test whether the stimuli found using the space-clamp software produced potentials capable of decrement-free propagation, we attempted to test our results with the PAP (propagating action potential) software. Although we converted all results into the units required by the PAP software, the two models are apparently incompatible, as they apply their holding currents differently. The current-clamp model applies the current over the entire axonal membrane ( $J_h$  is specified in  $\mu\text{A}/\text{cm}^2$ ), whereas the PAP model applies  $I_h$  only at a specified  $x$  value. Because this experiment observed the effects of an increased  $V_m^o$  due to increased  $J_h$ , the PAP software was of no use.

## 4.3 Controls

- *Action Potential Definition.* Although how we define an action potential greatly affects the results for Region C, it does not have a significant impact on regions A and B. Changing the definition of an action potential changes the absolute magnitudes of  $J_p$ , but the relative trends we observe are identical. Consequently, we can confidently say that the results for regions A and B are independent of action potential definition.
- *Numerics.* The step size and relative tolerance affect the accuracy with which the software simulates the application of the stimulus. We decreased the step size and relative tolerance by a factor of 10 and did not see significant changes in our data. Therefore, our results are probably not due to data calculation error.

- *Changing  $V_L$ .* Because the effect of changing the holding current was to change the resting membrane potential, the same results should occur if we only change  $V_m^o$ . To change  $V_m^o$ , we changed the leakage voltage  $V_L$ . The equivalent  $V_L$  leading to the same  $V_m^o$  for a holding current  $J_h$  was calculated as  $V_L = J_h/G_L + V_L^o$  where  $V_L^o$  was the original value of  $V_L$ . When we ran the simulations again changing  $V_L$  and without any holding current, we obtained exactly the same results, assuring us that the results are not due to the way the software handles holding currents.
- *Other Parameters.* We plotted the parameters  $m, n, h, \frac{dm}{dt}, \frac{dn}{dt}, \frac{dh}{dt}, G_{Na}, G_K, \frac{G_{Na}}{G_K}, J_{Na}, J_K, \frac{J_{Na}}{J_K}, \max(\frac{dG_{Na}}{dt}), \max(\frac{dG_K}{dt}), \max(\frac{dG_{Na}/dt}{dG_K/dt}), \text{average}(\frac{dG_{Na}}{dt}), \text{average}(\frac{dG_K}{dt}),$  and  $\text{average}(\frac{dG_{Na}/dt}{dG_K/dt})$  versus both  $V_m$  and  $J_h$ . None of these parameters contributed to an explanation of our results; there was no smooth trend as in the  $J_p$  v.  $J_h$  graph. Consequently, none of these variables, either alone or in any obvious combination, can explain the results seen.

## 4.4 Future Work

### 4.4.1 Software

The application of a holding current in the space-clamp software is highly questionable. The space-clamp software is supposed to start the simulation assuming that the holding current has been applied since  $t = -\infty$ , and thus conditions have already reached steady-state. We found that when we simulated a holding current by applying a very long duration pulse of amplitude  $100 \mu\text{A}/\text{cm}^2$ , we observed an oscillatory membrane voltage. Consequently, no steady-state membrane voltage could exist. However, when a software-defined holding current of  $100 \mu\text{A}/\text{cm}^2$  is applied, a steady-state is somehow found.

Future work could correct this flaw in the software, enabling it to recognize oscillatory or repetitive activity, and include this in its calculations of response to a pulse stimulus. Furthermore, we could change  $V_L$  in the PAP software to simulate a holding current applied along the length of the axon; this would allow us to use propagation as a criterion for action potential generation.

#### 4.4.2 Action Potential Definitions

Because the results for Region C are heavily dependent on the action potential definition, it is of the utmost importance to find a complete and correct definition. An in-depth analysis of the change of sodium and potassium conductance, or some interaction between the two, could be useful. This would also be helpful in explaining the jagged profile observed in Figure 5.

#### 4.5 Conclusion

Figures 4 and 5 shows that zero holding current is close to the point at which minimal stimulus is required to generate an action potential. This shows that the squid operates at a near optimum resting potential for generating action potentials. This experiment also supported our hypothesis for moderate holding currents: the pulse amplitude needed to stimulate a neuron increases with increased holding current. For extreme cases, the results were contrary to our hypothesis but our results may be inaccurate due to the problems described above. Furthermore, the results are difficult to explain in terms of our original idea of the underlying mechanism (a decrease in the initial value of  $dm/dt$ ). However, we found that the equilibrium-points model, while only an approximation, hints at the fundamental trends involved.

## References

- [1] T. F. Weiss, *Cellular Biophysics*, vol. 2. MIT Press, 1997.